Article ID: 1000-7032(2023)03-0496-12

Advances and Progress of Hybrid X-ray Detectors

ZONG Jia[1], LI Weijun[1], LIU Lulu[1], WEI Haotong[1,2*]

(1. *State Key Laboratory of Supramolecular Structure and Materials, College of Chemistry, Jilin University, Changchun* 130012, *China*;
2. *Optical Functional Theranostics Joint Laboratory of Medicine and Chemistry, The First Hospital of Jilin University, Changchun* 130012, *China*)

* *Corresponding Author, E-mail: hweichem@jlu. edu. cn*

Abstract: Dominating X-ray detectors are mainly divided into direct semiconductor X-ray detectors and indirect scintillator X-ray detectors. In recent years, hybrid X-ray detectors have emerged by combing the advantages of semiconductors and scintillators. The mixed semiconductors and scintillators as active layers lead to different working mechanisms. The charge/energy transfer between the two phases avoids the afterglow effect of the scintillator. And the presence of scintillators also optimizes the properties of the semiconductor material. The review summarizes the mechanism, progress, and synergistic effect of hybrid X-ray detectors to highlight the advances of hybrid X-ray detectors. Three types of hybrid X-ray detectors are discussed in detail according to different working mechanisms and their respective characteristics. Finally, we present an outlook on hybrid X-ray detectors' limitations and the future development direction.

Key words: hybrid X-ray detector; direct X-ray detection; indirect X-ray detection; working mechanism

CLC number: TL816. 1; O434. 1 **Document code**: A **DOI**: 10. 37188/CJL. 20220327

杂化X射线探测器的优势与进展

宗 佳[1], 李维俊[1], 刘璐璐[1], 魏浩桐[1,2*]

(1. 吉林大学 化学学院, 超分子结构与材料国家重点实验室, 吉林 长春 130012;
2. 吉林大学第一医院 医学与化学光功能诊疗联合实验室, 吉林 长春 130012)

摘要: 占主导地位的X射线探测器主要分为直接半导体型X射线探测器和间接闪烁体型X射线探测器。近年来,杂化X射线探测器通过结合半导体和闪烁体材料的优势而出现。作为活性层的混合半导体和闪烁体导致了不同的工作机制。两相之间电荷/能量转移可以避免闪烁体的余辉效应。并且闪烁体的存在也优化了半导体材料的性能。本文总结了杂化X射线探测器的机制、进展和协同效应,以突出杂化X射线探测器的优势。根据不同的工作机制和各自的特点,我们详细讨论了三种类型的杂化X射线探测器。最后,我们对杂化X射线探测器存在的局限性和未来的发展方向进行了展望。

关 键 词: 杂化X射线探测器; 直接X射线探测; 间接X射线探测; 工作机制

1 Introduction

Since the discovery of X-rays in 1895, the solid penetrating capability of X-ray has led to the widespread use of X-ray detectors in security screening, nondestructive detecting, and medical imaging[1-3]. Both the semiconductor-based direct X-ray detectors[4-5] and scintillator-based indirect X-ray detectors[6-7]

收稿日期: 2022-09-07; **修订日期**: 2022-09-22
基金项目: 国家自然科学基金(52173166); 中央高校、吉林大学和吉林科技学院基本科研业务费(2017TD-06)
Supported by National Natural Science Foundation of China(52173166); Fundamental Research Funds for the Central Universities, JLU and JLUSTIRT(2017TD-06)

develop very fast as the intensive research, mature material synthesis technology, and improved device fabrication processes.

Direct X-ray detectors employ semiconductors to directly convert X-rays photons into charge carriers[8-10]. Electrons and holes then drift to the opposite electrode ends under an electric field. Direct X-ray detectors offer better spatial resolution due to the absence of intermediate conversion processes. Amorphous silicon (α-Si) flat-panel[11] was first proposed with a PIN structure in 1993. Later, inorganic materials amorphous selenium (α-Se) were widely commercialized to enlarge the stopping power of Si[12-14], since the X-ray attenuation coefficient follows the relationship of $\alpha \propto Z^4/E^3$, where Z is the atomic number in the material, and E is the energy of the X-ray photon[15]. However, α-Se detectors have a limited lifetime under the high electric field of direct detection and their maintenance costs are high. In recent years, direct X-ray detectors based on cadmium telluride (CdTe) and cadmium zinc telluride (CdZnTe) semiconductors, which offer good energy resolution, have become very attractive in the field of imaging. However, large size and high-quality single crystals (*e. g.*, CdZnTe) are challenging to grow[16]. And it isn't easy to prepare flexible detectors from robust inorganic semiconductor materials[17]. Although low-cost wet processing techniques can fabricate large organic semiconductor materials[18], organics consisting of low atomic number elements have a weak attenuation of X-rays, resulting in limited sensitivity of direct X-ray detectors. Emerging perovskites with a structure of ABX_3 (A=Cs, formamide (FA), methylammonium (MA), B=Pb, Sn or Bi, X=Cl, Br or Ⅰ) have excellent properties of high X-ray attenuation coefficients, large carrier mobility-lifetime products ($\mu\tau$), and solution-processed single-crystal growth[19-22]. However, the dark current and noise induced by the perovskite ions migration severely limit the detection limit and operational stability of the device[23-24].

Indirect scintillator detectors first convert high-energy X-rays into visible photons, which are detected by the image sensor (photomultiplier tube (PMT), charge-coupled device (CCD), or complementary metal oxide semiconductor (CMOS)) to indirectly convert X-rays photons into electronic signals[25-27]. Indirect X-ray detectors, which are cheaper and more stable than direct detectors, have gained wide acceptance. Compared to inorganic crystal scintillators with harsh preparation conditions and organic crystal scintillations of weak stopping power, low light yield, and low transparency[28-30], perovskite scintillations possess strong X-ray stopping power, and the capability to produce color-tunable emission to enlarge the Stokes shift[31-33]. However, perovskite materials are less environmentally stable and are prone to phase changes under X-ray irradiation. And some perovskite scintillators (*e. g.*, $(PPN)_2SbCl_5$ (PPN=bis (triphenylphosphoranylidene) ammonium cation)[34], lead-free copper-based halide (Rb_2CuCl_3)[35]) are limited by the long afterglow (microsecond luminous lifetime), which often results in an ultralong response time. In addition, the light scattering problem of the indirect scintillator makes the device have a low spatial resolution, which is very disadvantageous for high-definition imaging[36-37].

Hybrid X-ray detectors are new kinds of solid X-ray sensors that combine the advantages of direct semiconductors and indirect scintillators[38-39]. For direct detection of semiconductor materials, strong X-ray attenuation is necessary. For indirect scintillator materials, avoidance of excessive light scattering and afterglow effects is necessary. Hybrid X-ray detectors can improve the sensitivity of semiconductor materials with weak X-ray attenuation coefficients while avoiding the light scattering and afterglow effects of scintillators. The advent of hybrid X-ray detectors has opened up the possibility of further development of many semiconductor and scintillator materials that are limited by their properties. However, hybrid X-ray detectors also suffer from a certain degree of deficiencies, such as phase stability and passivation of interface defects. Although hybrid X-ray detectors do not yet match perovskite direct X-ray detectors in terms of single performance (*e. g.*, sensitivity), they show good promise in terms of combined performance (combines flexibility, sensitivity, spatial resolution and response time).

In hybrid X-ray detectors, since organic molecules often have much smaller stopping power compared to the inorganic counterpart, inorganic scintillators are often employed to boost the scintillation processes[40-41]. The mixed semiconductor and scintillator serving as active layers lead to a different working mechanism. Type (Ⅰ) If the semiconductor is made of organic materials, X-ray induced charge carriers are mainly generated in the inorganic scintillator phase compared to the organic phase. Two pathways may occur during optoelectronic conversions. In one pathway, the emitting light from the scintillator can be absorbed by the semiconductor, and light-generated charges are transported along the semiconductor phase[42]. In the other pathway, charge or energy transfer occurs between the scintillator and semiconductor, followed by the same charges transport process[43]. The two pathways often compete with each other, and the final processes are determined by the two-phase architecture correlations and energy band structures. Type (Ⅱ) If the semiconductor is made of inorganic or heavy-element materials, charges can be generated within both the semiconductors and the scintillators[38]. Apart from the optoelectronic conversion processes, semiconductors can also directly attenuate the X-rays and contribute to the signal current.

It has been reported that the incorporation of scintillators into organic semiconductors can effectively solve the light crosstalk phenomenon of scintillators without affecting their luminescent properties[44]. And it has also been shown that the introduction of scintillator blocking layers in perovskite semiconductors can restrain the ion migration phenomenon of three-dimensional(3D) perovskites and avoid the light scattering effect of scintillators, thus improving the detection performance of the devices[38-39]. As a result, hybrid X-ray detectors that can break through the limitations of traditional scintillators through different mechanisms, and show good prospects for further development. In the following, we present a breakdown of the different operating mechanisms of hybrid X-ray detectors and explore their competitive advantages.

2 Working Mechanism of Hybrid X-ray Detectors

Three different working mechanisms of hybrid X-rays have been reported. When organic molecules, which exhibit weak absorption of X-rays, are used as semiconductor materials: (1) Scintillators convert X-rays directly into visible light, the organic semiconductor in the hybrid layer rapidly converts UV-visible photons into charge carriers. Compared to conventional scintillator photodetectors, hybrid detectors based on the working mechanism of Fig. 1(a) can effectively increase the photoelectric conversion efficiency. (2) As shown in Fig. 1(b), scintillators first attenuate the X-rays, and generate the charge carriers. Due to the favorable energy band structure, the charge carriers are completely transferrted to the adjacent semiconductor phase before radiative recombination[43]. The response time of this kind of device working on this principle is often on the order of nanoseconds range, hugely shortening the response

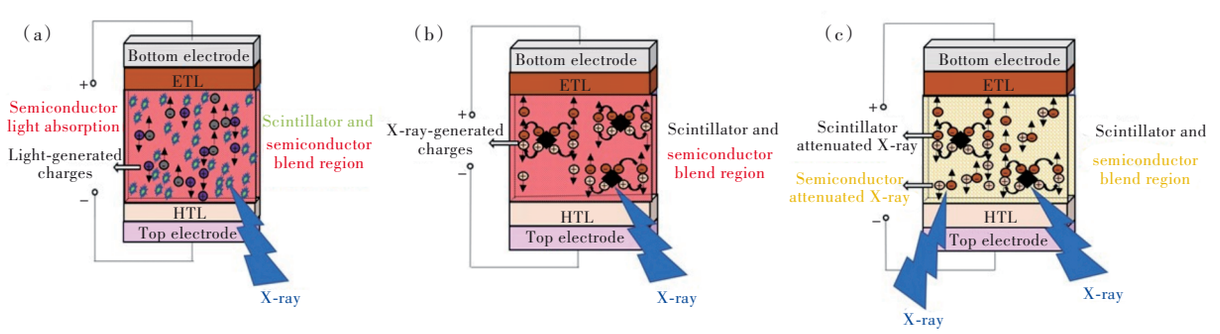

Fig.1 (a)Schematic of scintillation reabsorption to suppress light scattering in a hybrid X-ray detector. (b)Schematic diagram of the charge/energy transfer principle of scintillators in a hybrid X-ray detector. (c)Schematic diagram of the operation of a hybrid X-ray detector with multiple charge collection paths.

time of the scintillators[45-46]. Thus, many high efficient scintillators that have serious afterglow effects can be reconsidered based on this new device architecture. (3) When heavy elemental materials with strong X-ray attenuation serve as semiconductors in Fig. 1(c), semiconductors and scintillators that exhibit strong X-ray absorption allow two different charge collection paths in hybrid X-ray detector[38]. One is the direct attenuation of X-rays into charge carriers by the semiconductor. The other is the same as the working principle (2) (presence of charge transfer from scintillator).

3 Avoid Scintillation Reabsorption to Suppress the Light Scattering and Crosstalk

Although indirect scintillators coupled with photodetector arrays have been widely commercialized due to their convenience and low-cost advantages, conventional indirect X-ray detectors also have some fatal disadvantages, such as low sensitivity and poor spatial resolution. To avoid the optical crosstalk of scintillators, Büchele *et al.* [44] prepared a hybrid X-ray detector by incorporating terbium-doped gadolinium oxide (GOS: Tb) particles into the bulk heterojunction (BHJ) (see Fig. 2(a)) in 2015. GOS: Tb scintillators convert X-rays into visible photons, which are then absorbed by the adjacent BHJ, significantly reducing the optical crosstalk phenomenon. The sharpness comparison of the X-ray imaging in Fig. 2(b) further verifies the significant improved spatial resolution (4.8 lp·mm^{-1}). It should be noted that the filling amount of GOS: Tb is the key point, which should be below 66% as shown in Fig. 2(c) to maintain the continuity of the polymer phase and avoid any voids in the composite. Otherwise, the device

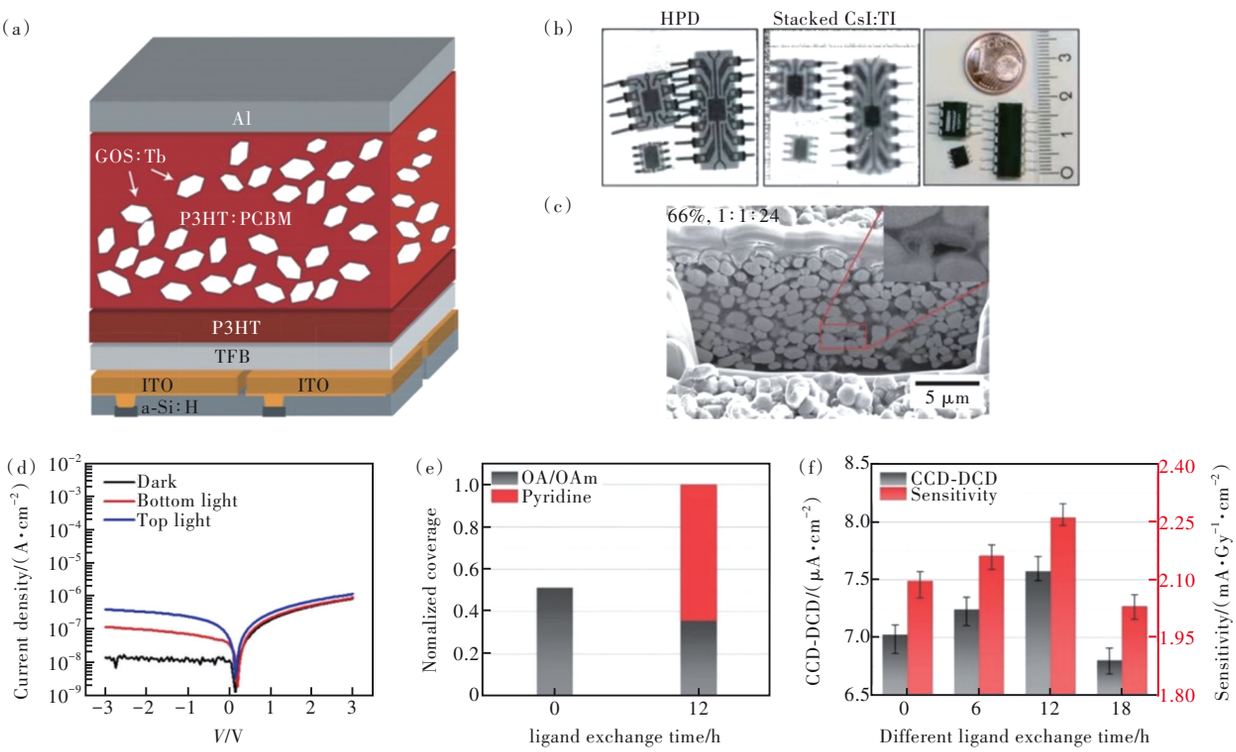

Fig.2 (a) Schematic of the image sensor with an a-Si: H backplane and a hybrid front-plane[44]. (b) 70 kV X-ray images of integrated circuit devices (photograph on the right) realized with an HPD image sensor (left) and a conventional stacked device (center)[44]. (c) SEM cross-sections (FIB cuts with 52° tilt angle), red boxes and insets highlight voids inside the devices[44]. (d) Current density curves of the device with a blending weight ratio of 1∶1∶2 *versus* bias voltage. The thicknesses of the active layer are about 20 μm. The 520 nm incident light at 146 μW·cm^{-2} enters from the top side (Al electrode) and the bottom side (ITO electrode), respectively[42]. (e) The normalized coverage ratio (OA/OAm- and pyridine capped) under the 0 and 12 h ligand exchange time[48]. (f) The evaluated parameters (RS, CCD-DCD, and sensitivity) of the detectors based on P3HT: PC71BM active layer with $FAPbBr_3$ QDs (1 mg) at 0, 6, 12, 18 h ligand exchange time[48].

will exhibit a high dark current of >100 nA·cm^{-2}.

To suppress the large leakage current, Xiang *et al.* [42] uniformly dispersed lead cesium bromide($CsPbBr_3$) perovskite quantum dots(QDs) into the BHJ in 2021, and the reduction of internal defects combined with the high efficiency of light yields(~95%) enables a detection sensitivity of 3.7 μC·Gy_{air}^{-1}·cm^{-2} while maintaining a low dark current(2.3 nA·cm^{-2}) of the hybrid X-ray detector. Further elevating the $CsPbBr_3$ QDs amount will cause the assembly of QDs at the device bottom, and the self-absorption prevents more visible light transmission to the semiconductor layer, thus weakening the performance of the hybrid X-ray detector(see Fig. 2(d)). To ensure that the incorporation of nanoparticles does not affect the phase stability of organic semiconductors, researchers often introduce organic ligands onto the surface of nanoparticles. The introduction of ligands improves the surface defects of QDs and also influences the properties and stability of the QDs. Kim *et al.* [47] demonstrated that introducing short-chain ligands on QDs facilitates active materials' dispersion and improves the charges transfer. Lee *et al.* [48] replaced the oleic acid/oil geshiamine (OA/OAm) ligands in the formamidine lead bromide ($FAPbBr_3$) QDs with short-chain pyridine ligands for high electrical conductivity(pyridine higher surface coverage in Fig. 2(e)). Although short-chain ligands with high electrical conductivity facilitate charge transport compared to long-chain ligands, there is major concern on the long-term stability in the coexistence between nanoparticles with organic phases. The ligand coating on the surface of the quantum dots will greatly affect the stability of the material. As shown in Fig. 2(f), the detection performance of the device drops significantly after 18 h of operation. Further research needs to balance the detection performance and operational stability of hybrid X-ray detectors.

4 Charge/Energy Transfer in Suppressing the Scintillator Afterglow

Afterglow is a common phenomenon of scintillators that describes the long radiative recombination lifetime of charge carriers. Many excellent scintillators have high scintillation efficiency but failed in commercial competition due to the scintillation afterglow effect, which can cause severe imaging smear and low spatial resolution. In contrast, hybrid X-ray detectors realize fast charge carrier/energy transfer from scintillators to semiconductors, thereby hugely reducing the response time of the device. Therefore, many synthesized scintillators that have high luminescent efficiency but long afterglow can be reevaluated due to the fast development of hybrid X-ray detectors. At the same time, the introduction of semiconductor materials into scintillators can improve the charge collection efficiency and avoid the light scattering effect, thereby increasing the sensitivity of the detector.

In 2016, Ankah *et al.* [43] introduced lead sulphide(PbS) quantum dots into organic heterojunctions(BHJs). The electrons and holes generated by PbS are transferred to the corresponding semiconductor phase without recombination of luminescence by the energy level structure(see Fig. 3(a)). In theory, a hybrid X-ray detector based on this working mechanism should exhibit fast response. However, the poor solubility of PbS particles leads to inhomogeneous mixing of the composite material, as shown in Fig. 3(b), and the response time of the device is severely affected as the active layer thickness increases. The bismuth oxide(Bi_2O_3) shows advantages in higher atomic numbers, strong stopping power, and non-toxic properties[49]. And the higher density of Bi_2O_3 facilitates adding small amounts of nanoparticles to meet high weight fractions, which contributes to the homogeneous dispersion of the active substance. In 2018, Thirimanne *et al.* [50] incorporated Bi_2O_3 nanoparticles(NPs) into the BHJ to construct an ITO/poly(3,4-ethylenedioxythiophene): poly(styrene-sulfonate) (PEDOT: PSS)/P3HT-PCBM-Bi_2O_3/BCP/Al hybrid X-ray detector. The nanoparticles were periodically and uniformly distributed in the mixed layer, forming a nanoscale diode close to the NPs and facilitating efficient charge extraction(>60%) by poly(3-hexylthiophene)(P3HT) and [6,6]-phenyl-

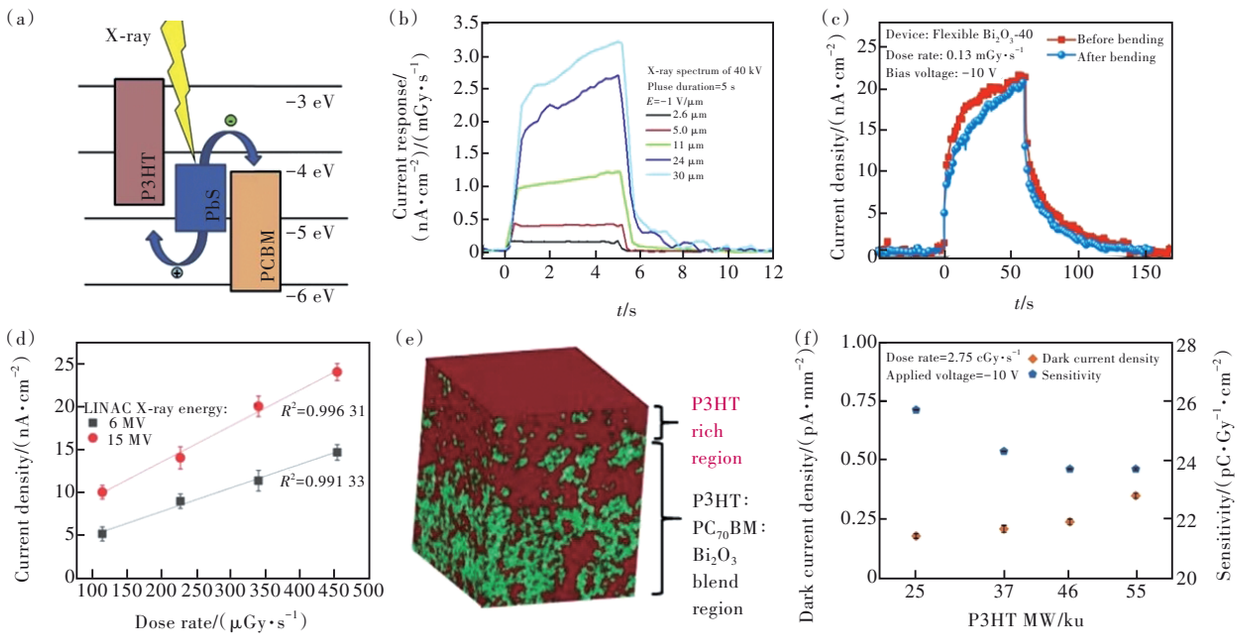

Fig.3　(a) Sketch of the "BHJ-HOMO LUMO" e charge generation and transport in the device[43]. (b) X-ray induced current response of the devices plotted as current density per dose rate *versus* time at an average dose rate of 10 mGy·s^{-1}[43]. (c) X-ray photocurrent response before and after bending for a flexible Bi_2O_3-40 device[50]. (d) Dose dependence of the hybrid X-ray detector under X-ray irradiation of 6 MV and 15 MV LINAC. All the devices are operated at −10 V. Active device area is 0.68 cm^2[50]. (e) Schematic of the NP-BHJ film illustrating the vertical composition gradient resulting in a P3HT rich top region and an organic-inorganic mixed bottom region[53]. (f) Dark current density and sensitivity of the NP-BHJ detectors as a function of P3HT MW[55].

C_{70}-butyric acid methyl ester (PCBM). The hybrid X-ray detector exhibits a sensitivity of 42.8 μC·Gy^{-1}·cm^{-2} and 1.5 μC·Gy^{-1}·cm^{-2} for "soft" and "hard" X-rays respectively. Moreover, the introduction of NPs does not affect the flexibility of the organic semiconductor. Fig. 3(c) shows that the sensitivity of the hybrid X-ray detector remains after a 3 mm radius bending for ten times. The hybrid X-ray detector exhibits a sensitivity of 7 μC·Gy^{-1}·cm^{-2} for flexible detection and the flexible performance has been developed to facilitate medical imaging. To enable practical application, the accuracy of the radiation dose of this hybrid X-ray detector exhibits a good linear response as shown in Fig. 3(d).

Although BHJ/NPs-based hybrid X-ray detectors achieved prominent breakthroughs in sensitivity and real-time response, the excessively high dark current of about 10^3 nA·cm^{-2} at a bias voltage of −10 V results in high detection dose rates and poor imaging clarity. It is known that the hygroscopic nature of PEDOT:PSS can disrupt the structure of the hole transport layer(HTL), resulting in poor charge selectivity of the X-ray detector[51-52]. Therefore, Nanayakkara *et al.* [53] developed the hybrid X-ray detector with the inverted device architecture of ITO/ZnO/Bi_2O_3-PCBM-P3HT/Ag in 2021. As shown in Fig. 3(e), the active material is distributed in a vertical gradient in the mixed layer, with an enrichment of the p-type semiconductor P3HT near the Ag electrode. The P3HT that accumulates near the anode region corresponds to a hole-selective/electron-blocking layer. P3HT effectively prevents electrons to transfer from the PCBM phase to the anode region, thus achieving an ultra-low dark current(the dark current density of the hybrid X-ray detector remains below the industry requirement of 1 nA·cm^{-2} even at high electric fields). To achieve medical dose accuracy, Nanayakkara *et al.* [53] also tested the angular dependence for the hybrid detector, displaying angular support of below 6% under irradiation with hard X-rays. HTL-free hybrid X-ray detector with inverted device structure can better fit variations in body shape and is

more conducive to accurate dose detection[54].

Compared to flat panel detectors, flexible detectors show better trends due to their greater flexibility and clarity in imaging. To further enhance the flexibility of the HTL-free BHJ/NPs hybrid X-ray detector while maintaining the detection performance, Nanayakkara *et al.* [55] investigated the effect of organic polymers' molecular weight (MW) on the device in 2022. The shorter chain length of the low MW P3HT favors a high degree of polymer crystallization, leading to a faster migration rate of carriers and improving device sensitivity (see Fig. 3(f)). However, the high crystallinity of organic polymers is detrimental to the mechanical flexibility of the device. By modulating the molecular weight of the organic semiconductor, the hybrid X-ray detector based on P3HT (>40 ku)/PCBM/Bi_2O_3 has been further improved in flexibility while maintaining the original ultra-low dark current (<0.1 nA·cm^{-2}). This suggests that with further optimization, a highly sensitive flexible semiconductor/scintillator-based X-ray detector is achievable.

5 Multi-charge-collection Paths in Perovskite/Scintillator Hybrid X-ray Detector

Halide perovskites possess high X-ray attenuation coefficients and high charge carrier mobility, which efficiently extracts the X-ray induced charges from inside bulk crystals. The excellent properties of halide perovskites are incredibly beneficial for high-quality direct detection. However, perovskites are easily degraded by the environment, which is still a major concern. In indirect detection, scintillators with decay lifetimes of more than microseconds have severe afterglow phenomena, making them difficult to utilize. In 2021, Li *et al.* [38] prepared the perovskite semiconductor/scintillator hybrid X-ray detector through a tableting process, which was demonstrated to be an excellent solution to the afterglow through fast energy transfer process. Fig. 4(a) shows that the ethylenebis-triphenylphosphonium manganese (Ⅱ) bromide ($(C_{38}H_{34}P_2)MnBr_4$) scintillator is uniformly dispersed at the grain boundaries of the

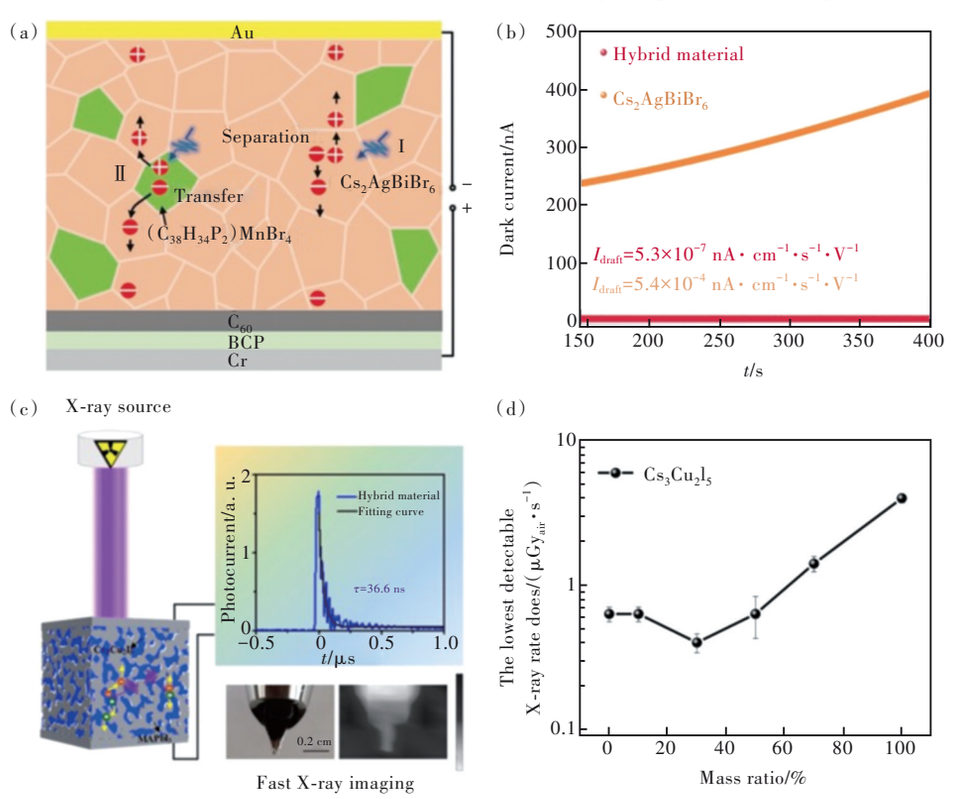

Fig.4 (a) Schematic mechanism of the $Cs_2AgBiBr_6/(C_{38}H_{34}P_2)MnBr_4$ hybrid detector[38]. (b) Dark drift current of the hybrid material and $Cs_2AgBiBr_6$ device[38]. (c) Fast X-ray imaging ability of the $MAPbI_3/Cs_3Cu_2I_5$ hybrid X-ray detector[39]. (d) The lowest detectable X-ray rate does of the hybrid devices with different scintillator contents[39].

cesium silver bismuth bromide ($Cs_2AgBiBr_6$) perovskite, thus effectively blocking the ion migration channel of the perovskite. Therefore, compared to the $Cs_2AgBiBr_6$ perovskite semiconductor-based X-ray detector, the dark current drift of the $Cs_2AgBiBr_6$/($C_{38}H_{34}P_2$) $MnBr_4$ hybrid detector is significantly suppressed (see Fig. 4(b)), which is beneficial for hard X-ray detection. Liu *et al.* [39] optimized the device structure and prepared Au/2,2′,7,7′-tetra[N,N-bis (4-methoxyphenyl) amino] -9, 9′-spirobifluorene (Spiro-MeOTAD)/$MAPbI_3$/methylamine lead iodide ($MAPbI_3$)-cesium copper iodide ($Cs_3Cu_2I_5$)/$MAPbI_3$/C_{60}/bathocuproine (BCP)/Cr hybrid X-ray detectors in 2022. Covering both sides of the hybrid layer with a thin perovskite phase reduces fugitive photoluminescence (PL) emission from the surface of active layers and helps collect more charge carriers. The $MAPbI_3$/$Cs_3Cu_2I_5$-based hybrid X-ray detector shows a fast response time (36.6 ns) compared to the long decay lifetime of the $Cs_3Cu_2I_5$ scintillator (1.07 μs). This is because all the charge generated by the scintillator's attenuated X-rays will be transferred to the semiconductor phase under the barrier effect of the type Ⅱ heterojunction constructed by the scintillator and the semiconductor material. The uncharged recombination of the luminescence process facilitates the device to exhibit a nanoscale response and the nanosecond response time of the X-ray detector is advantageous for dynamic scanning at multiple angles for medical purposes, and Fig. 4(c) demonstrates the potential of the perovskite semiconductor/scintillator hybrid X-ray detector for fast imaging.

Sensitivity and detection limits are crucial figures-of-merit for X-ray detectors. Although semiconductor-based direct X-ray detectors are extremely sensitive, they require a high cost for high-quality single crystals. Since the ion migration of 3D perovskites and scintillators' light scattering are effectively suppressed, the $MAPbI_3$/$Cs_3Cu_2I_5$ hybrid X-ray detector shows a high sensitivity of 885 $\mu C \cdot Gy_{air}^{-1} \cdot cm^{-2}$ and a low detection limit of 0.41 $\mu Gy_{air} \cdot s^{-1}$ under hard X-ray operated at 120 kV condition (see Fig. 4(d)). Perovskite semiconductor/scintillator hybrid X-ray detectors show excellent performance for practical applications. The detection performance of three hybrid X-ray detectors with different working mechanisms are compared in Tab.1.

Tab. 1　Performance of hybrid X-ray detectors based on different materials

Hybrid layer	Voltage/V	X-ray energy/kV	Dark current/($nA \cdot cm^{-2}$)	Sensitivity/($\mu C \cdot Gy_{air}^{-1} \cdot cm^{-2}$)	Detection limit/($\mu Gy_{air} \cdot s^{-1}$)	Refs
PTAA/Bi_2O_3 NPs	−150	50	1.0	4.0×10^{-1}	1.3×10^{4}	[49]
P3HT/PCBM/PbS QDs	−30	40	~110	1.3×10^{-1}	—	[43]
	−10	50	~ 10^3	48	27	[50]
	−200	70	~ 10^5	1.6×10^{4}	20	[56]
P3HT/PCBM/Bi_2O_3 NPs	−10	6.0×10^{3}	—	30.8	114	[54]
	−100	70	1.0	1.5×10^{3}	56.7	[53]
	−10	6.0×10^{3}	~0.1	1.7×10^{-1}	1.5	[55]
P3HT/PCBM/GOS:Tb	−10	70	~ 10^2	5.8	1.5×10^{3}	[44]
P3HT/PCBM/$CsPbBr_3$ QDs	−3	40 ~ 80	2.3	3.7	5.8×10^{2}	[42]
$Cs_2AgBiBr_6$/($C_{38}H_{34}P_2$)$MnBr_4$	−100	120	0.4	114	0.2	[38]
$MAPbI_3$/$Cs_3Cu_2I_5$	−100	120	—	885	0.4	[39]

6　Conclusion and Outlook

New types of hybrid X-ray detectors are discussed to show their advantages in improving the shortcoming of scintillators in this minireview. Semiconductor materials in hybrids can provide additional charge collection paths and multi-charges generation processes depending on the stopping power of semiconductors. Because of the weak X-ray absorption of organic semiconductors, the organic/scintillator hybrid

detectors can generate X-ray induced charges mainly in scintillator phase, but organic phase can provide flexible properties. Perovskites, because of their excellent X-ray attenuation capabilities, allow for a direct X-ray attenuation way as semiconductor phase except the scintillator-absorbing path. The two charges collection paths allow for X-ray detectors' higher energy conversion efficiency.

With the development of society, people are no longer satisfied with bulky and complex detection equipment but prefer lightweight and flexible X-ray detectors[57]. Especially for medical radiotherapy, bulky instruments do not fit perfectly into the shape of the human body[58]. Organic/inorganic hybrid X-ray detectors with a linear X-ray dose-response, low beam angle dependence, and flexibility show promising trends in medical imaging and dosimetry. Although perovskite semiconductor/scintillator hybrid X-ray detectors show excellent potential in terms of sensitivity and detection limits, further research is needed to develop flexibility. In summary, hybrid X-ray detectors show ground-breaking advantages in terms of sensitivity, spatial resolution, response time and detection limits. Especially the charge/energy transfer process solves the afterglow phenomenon of many scintillators and largely reduces the device response time. However, the problem of homogeneous stability of the hybrid phase of hybrid X-ray detectors is currently a pressing one. Two-phase materials that are energy level matched and do not react with each other are necessary. For organic semiconductors, the choice of the right ligand modification is important. For three-dimensional perovskite semiconductors, ion migration is the main culprit for unstable device operation. The introduction of scintillators only weakly mitigates this phenomenon. So from the source we can choose some perovskite materials with good stability(*e. g.*, bismuth-based halide perovskites). Also, the relative content of semiconductors and scintillators is essential to control the stability of the mixed phase.

Current detectors still have deficiencies in terms of considerable size, mechanical flexibility, sensitivity to X-ray dose, and operational stability. Moreover, in order to gain a firm foothold in the detector market, hybrid X-ray detectors, which do not offer outstanding single detection performance, are in urgent need of further breakthroughs. In addition to improving the stability of the mixed phase, modification of the device structure and passivation of interfacial defects can be very helpful in improving detector performance[59]. The review will help readers understand the different working mechanisms of hybrid X-ray detectors and facilitate researchers' further development of hybrid X-ray detectors with excellent overall performance. More functions like digital, integrated, and smart are the critical high-tech cores to be developed in the future.

Response Letter is available for this paper at: http://cjl. lightpublishing. cn/thesisDetails#10. 37188/CJL. 20220327.

References:

[1] ROWLANDS J A. Material change for X-ray detectors [J]. *Nature*, 2017, 550(7674): 47-48.

[2] SPAHN M. X-ray detectors in medical imaging [J]. *Nucl. Instrum. Methods Phys. Res. Sect.* A *Accel. Spectrom. Detect. Assoc. Equip.*, 2013, 731: 57-63.

[3] LI Z Z, ZHOU F G, YAO H H, *et al*. Halide perovskites for high-performance X-ray detector [J]. *Mater. Today*, 2021, 48: 155-175.

[4] DANIELSSON M, PERSSON M, SJÖLIN M. Photon-counting X-ray detectors for CT [J]. *Phys. Med. Biol.*, 2021, 66(3): 03TR01-1-35.

[5] SCOTT C C, FARRIER M, LI Y, *et al*. High-energy micrometre-scale pixel direct conversion X-ray detector [J]. *J. Synchrotron Radiat.*, 2021, 28(4): 1081-1089.

[6] OLIVEIRA J, CORREIA V, COSTA P, *et al*. Stretchable scintillator composites for indirect X-ray detectors [J]. *Compos. Part* B *Eng.*, 2018, 133: 226-231.

[7] ZOU T Y, XIANG B, XU Y B, *et al.* Pixellated perovskite photodiode on IGZO thin film transistor backplane for low dose indirect X-ray detection [J]. *IEEE J. Electron Devices Soc.*, 2021, 9: 96-101.

[8] WEI H T, FANG Y J, MULLIGAN P, *et al.* Sensitive X-ray detectors made of methylammonium lead tribromide perovskite single crystals [J]. *Nat. Photonics*, 2016, 10(5): 333-339.

[9] SONG X, LI Q, HAN J, *et al.* Highly luminescent metal-free perovskite single crystal for biocompatible X-ray detector to attain highest sensitivity [J]. *Adv. Mater.*, 2021, 33(36): 2102190-1-10.

[10] ZHENG X J, ZHAO W, WANG P, *et al.* Ultrasensitive and stable X-ray detection using zero-dimensional lead-free perovskites [J]. *J. Energy Chem.*, 2020, 49: 299-306.

[11] STREET R. Semiconductor of distinction [J]. *Phys. World*, 1993, 6(4): 54-60.

[12] KASAP S O. X-ray sensitivity of photoconductors: application to stabilized a-Se [J]. *J. Phys.* D *Appl. Phys.*, 2000, 33(21): 2853-2865.

[13] KASAP S, FREY J B, BELEV G, *et al.* Amorphous and polycrystalline photoconductors for direct conversion flat panel X-ray image sensors [J]. *Sensors*, 2011, 11(5): 5112-5157.

[14] JIANG H, ZHAO Q H, ANTONUK L E, *et al.* Development of active matrix flat panel imagers incorporating thin layers of polycrystalline HgI_2 for mammographic X-ray imaging [J]. *Phys. Med. Biol.*, 2013, 58(3): 703-714.

[15] EVANS R D, BEISER A. The atomic nucleus [J]. *Phys. Tod.*, 1956, 9(12): 33.

[16] MAINPRIZE J G, FORD N L, YIN S, *et al.* A CdZnTe slot-scanned detector for digital mammography [J]. *Med. Phys.*, 2002, 29(12): 2767-2781.

[17] YUAN Y H, XIE S P, DING C G, *et al.* Fabricating flexible wafer-size inorganic semiconductor devices [J]. *J. Mater. Chem.* C, 2020, 8(6): 1915-1922.

[18] PEI K. Recent advances in molecular doping of organic semiconductors [J]. *Surf. Interfaces*, 2022, 30: 101887-1-5.

[19] WANG D L, CUI H J, HOU G J, *et al.* Highly efficient light management for perovskite solar cells [J]. *Sci. Rep.*, 2016, 6: 18922-1-10.

[20] SAIDAMINOV M I, ABDELHADY A L, MURALI B, *et al.* High-quality bulk hybrid perovskite single crystals within minutes by inverse temperature crystallization [J]. *Nat. Commun.*, 2015, 6: 7586-1-6.

[21] OGA H, SAEKI A, OGOMI Y, *et al.* Improved understanding of the electronic and energetic landscapes of perovskite solar cells: high local charge carrier mobility, reduced recombination, and extremely shallow traps [J]. *J. Am. Chem. Soc.*, 2014, 136(39): 13818-13825.

[22] LI W, XIN D Y, TIE S J, *et al.* Zero-dimensional lead-free $FA_3Bi_2I_9$ single crystals for high-performance X-ray detection [J]. *J. Phys. Chem. Lett.*, 2021, 12(7): 1778-1785.

[23] MCGOVERN L, GRIMALDI G, FUTSCHER M H, *et al.* Reduced barrier for ion migration in mixed-halide perovskites [J]. *ACS Appl. Energy Mater.*, 2021, 4(12): 13431-13437.

[24] LIU Y T, IEVLEV A, COLLINS L, *et al.* Operando imaging of ion migration in metal halide perovskites [J]. *Microsc. Microanal.*, 2020, 26(S2): 2046-2048.

[25] CAO J T, GUO Z, ZHU S, *et al.* Preparation of lead-free two-dimensional-layered $(C_8H_{17}NH_3)_2SnBr_4$ perovskite scintillators and their application in X-ray imaging [J]. *ACS Appl. Mater. Interfaces*, 2020, 12(17): 19797-19804.

[26] ZHANG Y H, SUN R J, OU X Y, *et al.* Metal halide perovskite nanosheet for X-ray high-resolution scintillation imaging screens [J]. *ACS Nano*, 2019, 13(2): 2520-2525.

[27] BELLAZZINI R, SPANDRE G, BREZ A, *et al.* Chromatic X-ray imaging with a fine pitch CdTe sensor coupled to a large area photon counting pixel ASIC [J]. *J. Instrum.*, 2013, 8(2): C02028-1-10.

[28] LEE H S, BHANG H, CHOI J H, *et al.* A search for low-mass dark matter with CsI(Tl) crystal detectors [J]. *Phys. Rev.* D, 2014, 90(5): 052006-1-6.

[29] CHA B K, KIM J Y, KIM T J, *et al.* Fabrication and imaging characterization of high sensitive CsI(Tl) and Gd_2O_2S(Tb) scintillator screens for X-ray imaging detectors [J]. *Radiat. Meas.*, 2010, 45(3-6): 742-745.

[30] BUGBY S L, JAMBI L K, LEES J E. A comparison of CsI:Tl and GOS in a scintillator-CCD detector for nuclear medicine imaging [J]. *J. Instrum.*, 2016, 11(9): P09009-1-13.

[31] GILL H S, ELSHAHAT B, KOKIL A, *et al.* Flexible perovskite based X-ray detectors for dose monitoring in medical imaging applications [J]. *Phys. Med.*, 2018, 5: 20-23.

[32] MAITI A, PAL A J. Effect of cation occupancy ordering in double perovskites to overcome hurdles in carrier transport: $Cs_2AgBiBr_6$ as a case study [J]. *J. Phys. Chem.* C, 2021, 125(29): 16324-16333.

[33] XU L J, LIN X S, HE Q Q, *et al*. Highly efficient eco-friendly X-ray scintillators based on an organic manganese halide [J]. *Nat. Commun.*, 2020, 11(1): 4329-1-7.

[34] HE Q Q, ZHOU C K, XU L J, *et al*. Highly stable organic antimony halide crystals for X-ray scintillation [J]. *ACS Mater. Lett.*, 2020, 2(6): 633-638.

[35] YANG B, YIN L X, NIU G D, *et al*. Lead-free halide Rb_2CuBr_3 as sensitive X-ray scintillator [J]. *Adv. Mater.*, 2019, 31(44): 1904711-1-8.

[36] LI Y, SHAO W Y, OUYANG X P, *et al*. Scintillation properties of perovskite single crystals [J]. *J. Phys. Chem.* C, 2019, 123(28): 17449-17453.

[37] MA W B, JIANG T M, YANG Z, *et al*. Highly resolved and robust dynamic X-ray imaging using perovskite glass-ceramic scintillator with reduced light scattering [J]. *Adv. Sci.*, 2021, 8(15): 2003728-1-8.

[38] LI W J, LIU L L, TAN M R, *et al*. Low-cost and large-area hybrid X-ray detectors combining direct perovskite semiconductor and indirect scintillator [J]. *Adv. Funct. Mater.*, 2021, 31(51): 2107843-1-9.

[39] LIU L L, LI W J, FENG X P, *et al*. Energy transfer assisted fast X-ray detection in direct/indirect hybrid perovskite wafer [J]. *Adv. Sci.*, 2022, 9(15): 2103735-1-8.

[40] LI H Y, SONG J M, PANG W T, *et al*. Sensitive and stable 2D perovskite single-crystal X-ray detectors enabled by a supramolecular anchor [J]. *Adv. Mater.*, 2020, 8(32): 2003790.

[41] NAGARKAR V V, GAYSINSKIY V, OVECHKINA E E, *et al*. Suppression of afterglow in CsI(Tl) by codoping with Eu^{2+}: fabrication of microcolumnar films for high-resolution high-speed imaging [J]. *IEEE Trans. Nucl. Sci.*, 2007, 54(4): 1378-1382.

[42] XIANG L, HUANG X K, WANG Y, *et al*. X-ray sensitive hybrid organic photodetectors with embedded $CsPbBr_3$ perovskite quantum dots [J]. *Org. Electron.*, 2021, 98: 106306-1-7.

[43] ANKAH G N, BÜCHELE P, POULSEN K, *et al*. PbS quantum dot based hybrid-organic photodetectors for X-ray sensing [J]. *Org. Electron.*, 2016, 33: 201-206.

[44] BÜCHELE P, RICHTER M, TEDDE S F, *et al*. X-ray imaging with scintillator-sensitized hybrid organic photodetectors [J]. *Nat. Photonics*, 2015, 9(12): 843-848.

[45] YAPARPALVI R, FONTENLA D P, VIKRAM B. Clinical experience with routine diode dosimetry for electron beam radiotherapy [J]. *Int. J. Radiat. Oncol. Biol. Phys.*, 2000, 48(4): 1259-1265.

[46] LNTANIWET A, MILLS C A, SHKUNOV M, *et al*. Characterization of thick film poly(triarylamine) semiconductor diodes for direct x-ray detection [J]. *J. Appl. Phys.*, 2009, 106(6): 064513-1-7.

[47] KIM S, LEE J, KANG J. Sensitivity improvement of quantum dot-blended hybrid detector for X-ray imaging [J]. *Coatings*, 2020, 10(3): 222-1-10.

[48] LEE K, LEE J, HAN D, *et al*. A study on improving the sensitivity of indirect X-ray detectors by adding hybrid perovskite quantum dots [J]. *Coatings*, 2022, 12(4): 492-1-11.

[49] INTANIWET A, MILLS C A, SHKUNOV M, *et al*. Heavy metallic oxide nanoparticles for enhanced sensitivity in semiconducting polymer X-ray detectors [J]. *Nanotechnology*, 2012, 23(23): 235502-1-7.

[50] THIRIMANNE H M, JAYAWARDENA K D G I, PARNELL A J, *et al*. High sensitivity organic inorganic hybrid X-ray detectors with direct transduction and broadband response [J]. *Nat. Commun.*, 2018, 9(1): 2926-1-10.

[51] DE JONG M P, VAN IJZENDOORN L J, DE VOIGT M J A. Stability of the interface between indium-tin-oxide and poly(3,4-ethylenedioxythiophene)/poly(styrenesulfonate) in polymer light-emitting diodes [J]. *Appl. Phys. Lett.*, 2000, 77(14): 2255-2257.

[52] SALSBERG E, AZIZ H. Degradation of PEDOT:PSS hole injection layers by electrons in organic light emitting devices [J]. *Org. Electron.*, 2019, 69: 313-319.

[53] NANAYAKKARA M P A, MATJAČIĆ L, WOOD S, *et al*. Ultra-low dark current organic-inorganic hybrid X-ray detectors [J]. *Adv. Funct. Mater.*, 2021, 31(8): 2008482-1-14.

[54] THIRIMANNE H M, JAYAWARDENA K D G I, NISBET A, *et al*. Hybrid multipixel array X-ray detectors for real-time direct detection of hard X-rays [J]. *IEEE Trans. Nucl. Sci.*, 2020, 67(10): 2238-2245.

[55] NANAYAKKARA M P A, MASTEGHIN M G, BASIRICÒL, *et al.* Molecular weight tuning of organic semiconductors for curved organic-inorganic hybrid X-ray detectors [J]. *Adv. Sci.*, 2022, 9(2): 2101746-1-15.

[56] JAYAWARDENA K D G, THIRIMANNE H M, TEDDE S F, *et al.* Millimeter-scale unipolar transport in high sensitivity organic-inorganic semiconductor X-ray detectors [J]. *ACS Nano*, 2019, 13(6): 6973-6981.

[57] 孙锡娟, 夏梦玲, 许银生, 等. 钙钛矿直接型X射线探测成像研究进展 [J]. 发光学报, 2022, 43(7): 1014-1026.
SUN X J, XIA M L, XU Y S, *et al.* Research progress of perovskite direct X-ray imaging [J]. *Chin. J. Lumin.*, 2022, 43(7): 1014-1026. (in Chinese)

[58] 郭素文, 杨伟峰, 胡云浩, 等. 硫化锌电致发光材料在智能可穿戴领域研究进展 [J]. 发光学报, 2022, 43(5): 796-806.
GUO S W, YANG W F, HU Y H, *et al.* Progress of zinc sulfide electroluminescent materials in intelligent wearable field [J]. *Chin. J. Lumin.*, 2022, 43(5): 796-806. (in Chinese)

[59] CHEN Y, YANG Z, WANG S B, *et al.* Design of an inorganic mesoporous hole-transporting layer for highly efficient and stable inverted perovskite solar cells [J]. *Adv. Mater.*, 2018, 30(52): 1805660-1-9.

宗佳(2000-),女,吉林松原人,硕士研究生,2022年于延边大学获得学士学位,主要从事钙钛矿光电探测的研究。
E-mail: weihaotong158@126.com

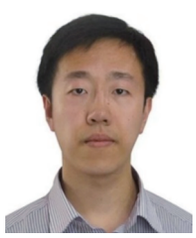

魏浩桐(1986-),男,吉林四平人,博士,教授,博士生导师,2014年于吉林大学获得博士学位,主要从事钙钛矿材料设计、制备及光电探测和X射线探测等方向的研究。
E-mail: hweichem@jlu.edu.cn